ASTRONOMY & ASTROPHYSICS
SUPPLEMENT SERIES

Astron. Astrophys. Suppl. Ser. **95**, 589-601 (1992)

Spectroscopic study of the atmospheric eclipsing binary VV Cephei*

M. Hack[1,3], S. Engin[2], N. Yilmaz[2], G. Sedmak[1,3,4], L. Rusconi[1,3] and C. Boehm[4]

[1] Department of Astronomy of the Trieste University, Via Tiepolo 11, I-34131 Trieste, Italy
[2] Department of Astronomy of the Ankara University, Besevler, Ankara, Turkey
[3] CIRAC (Interuniversity Regional Center for Astrophysics and Cosmology), c/o ISAS, Via Beirut 2, I-34013 Trieste, Italy
[4] Astronomical Observatory of Trieste, Via Tiepolo 11, I-34131 Trieste, Italy

Received December 20, 1991; accepted February 5, 1992

Abstract. — We present the results of the study of 49 high dispersion spectrograms obtained at the Haute-Provence Observatory from July 1967 to January 1981, including the epoch of the eclipse of 1977. The radial velocity, intensity and profile variations of several absorption and emission lines are given. The ratio between the fluxes of the M2 giant and the hot companion *versus* the wavelength indicates that the temperature of the latter is about 10000 K, confirming the results previously obtained from the study of ultraviolet IUE spectra. Another confirmation is given by the complete absence of He I lines in the spectrum of the companion, which is obtained by subtracting the M2 spectrum obtained during totality from the composite spectrum obtained completely out of eclipse.

Key words: VV Cephei: spectroscopy: stars: binaries: close

1. Introduction.

The atmospheric eclipsing binary VV Cephei exhibits a more complicated scenario than the other eclipsing binaries of the same class, with changes in emission and absorption features suggesting the presence of a very extended envelope surrounding the whole system, and perhaps an accretion disk around the hot companion. The spectral class and luminosity of the latter (star or accretion disk) were very poorly known, with estimates ranging between an O and an A-type, until ultraviolet observations were made with IUE.

We have studied all the IUE images collected between May 1978 and December 1984 (Hack *et al.* 1989) and derived the interstellar extinction from the depression at 2180 A: $E(B-V) = 0.40$. From the reddening corrected flux distribution we have derived a spectral type A0II. Although the resonance doublets of CIV and Si IV are present in the far ultraviolet, the complete absence of He I lines in the visual confirms that the spectral type of the companion is later than B5. A study of the ultraviolet spectrum observable from the ground, made by Struve (1944), also confirms that the companion is not very hot, because only absorption lines of once ionized metals are present. Actually the presence of hot signatures like CIV and Si IV is not unusual in interacting binaries with cool components: the very fact that the companion is moving in the extended envelope of the primary (as shown in Sect. 3) could explain the heating of the gas in the envelope itself.

2. The observations.

Several high dispersion spectrograms have been obtained (mainly by Faraggiana) with the coudé spectrographs of the 152 and 193 cm telescopes of the Haute-Provence Observatory (OHP) from July 1967 to September 1980. The epochs and phases, counted from the epoch of mid-primary eclipse are given in Table 1. Our purposes are: to compare the results of the 1975-1977 eclipse with those obtained during the previous eclipses of 1955-57 by Wright and collaborators (Wright 1970; Wright & Larson 1969; Wright 1977) and of 1935-37 by Goedicke (1939) and by Peery (1966), to study the radial velocity curves of the absorption and emission lines and their intensity variation, and to derive the ratio of the fluxes F_B/F_M by comparing the spectra obtained in the vicinity of the quadratures and at primary minimum.

Unfortunately we could not obtain spectrograms at the phases included between 0.18 and 0.50.

* Based on data obtained at the 193 and 152 cm telescopes of the Haute Provence Observatory. The data analysis has been performed at the ASTRONET pole of the Trieste Astronomy Department and Astronomical Observatory.

From a preliminary inspection of the spectra, the results obtained by previous investigators are confirmed:

1) the M-type spectrum dominates at wavelengths longer than Hδ. The only signature of the hot companion is the Balmer emission series. No Balmer discontinuity is observable at the limit of the Balmer series, suggesting that the emission continuum is produced by the extended envelope.

2) During totality the emissions at Hδ and at the upper terms of the series disappear completely; they almost disappear at Hγ and Hβ, while the emission is weak but present at Hα. At phases 0.95 and 0.04 the emission is present at Hδ. Out of eclipse the Balmer lines present two emission wings with the ratio R/V always being less than 1.

3) The FeII and [FeII] emissions are always present.

In the following Sections 3 to 6 we compare the radial velocities of various groups of lines with the orbital velocity curves for the M giant and the companion derived by Wright (1977).

3. H and K absorption lines of Ca II.

The radial velocity curve between phases 0.00 and 0.16 is parallel to that of the M supergiant, but more negative by about 20-25 km/s; at phases included between 0.5 and 0.0 is parallel to that of the companion, but more negative by about 20-25 km/s.

Both lines of Ca II present also two absorption components with radial velocities more positive than the main component by several tens of km/s (Fig. 1). What does this behavior mean?

A possible interpretation is suggested by consideration of the orbital circumstances. Between phases 0.0 and 0.17, the angular separation of the two stars is small and the main components of the CaII doublet can be formed in the extended atmosphere of the M star expanding at about 20 km/s, and absorbing the light of the hot companion (Fig. 2). The red-shifted components can be formed in streams directed toward the companion. At phases between 0.5 and 0.9, the shape of the RV curve suggests that the lines are formed in the envelope which is associated with, and maybe trailed by the hot companion, and is expanding at a velocity of 20-25 km/s relatively to its surface; the red shifted components could be formed in streams moving from the M star toward the companion at a velocity of 50-70 km/s.

Another possible interpretation is suggested by the work of Reimers & Schroeder (1989). They have observed the relation between the stellar radial velocity and the velocity of the circumstellar Ca II K line for six red giant spectroscopic binaries. Their main result is that the Ca II CS lines follow the stellar RV curve with different phase-delay and amplitude, when the ratio between the stellar wind velocity and the orbital K velocity is small,

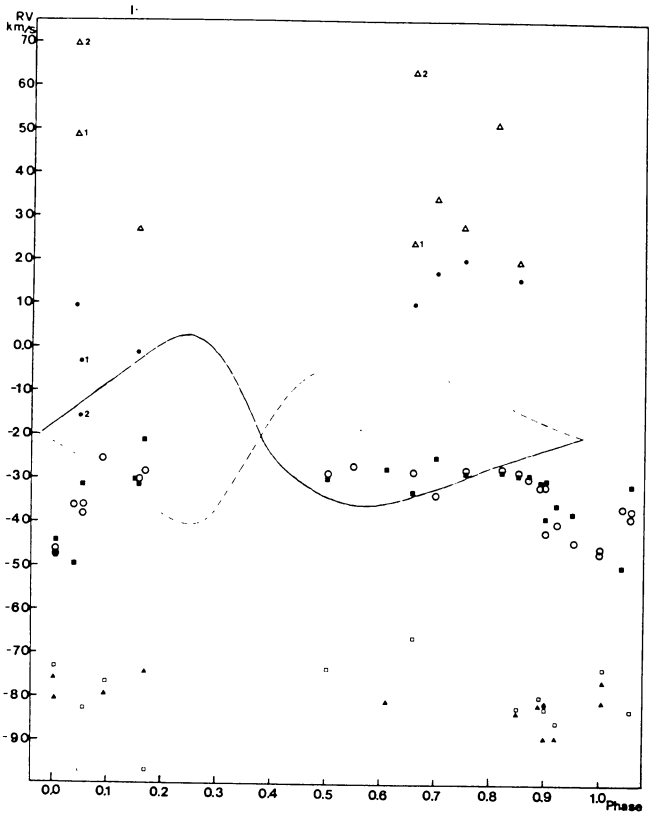

FIGURE 1. Radial velocities of the H and K Ca II lines. The orbital velocity curves for the M star (full line) and for the companion (dashed line) (Wright 1977) are plotted for comparison. The symbols mean: main H absorption (o), main K absorption (■), two secondary absorption components of H(•) and K(Δ), H(□) and K(Δ) violet emission wings.

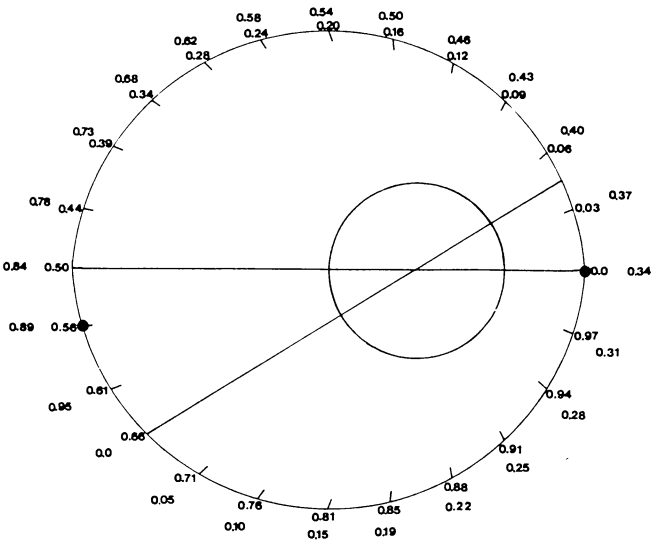

FIGURE 2. The orbit of the companion, according to Wright (1977). The phases counted from mid-eclipse and from epoch of passage at the periastron are given.

i.e. less than about 3, while no wind RV modulation is found for large values of this ratio. We have compared the results for VV Cephei given in Table 2, with their data (Table 6 of their paper).

Table 2 shows that the H and K CS lines and the Hα absorption core give the same parameters for the wind. VV Cephei, like the other stars having similar values of the ratio v_{wind}/K shows similar values of the angular phase displacement and a relatively small distance of the absorbing material in the line of sight from the star surface, measured in stellar radii. This result for VV Cephei indicates that the shell radius [that is the height where τ (Ca II) in the wind is about equal to 1] is 1.6 times larger than a sini; therefore the companion is moving inside the wind.

The modulation and phase displacement hypothesis can explain the behavior of the Ca II radial velocity curve at phases 0.0 to 0.17, but not that between phases 0.5 and 0.9.

The violet emission wings indicate RV ranging between −70 and −80 km/s; they are independent of the phase and roughly constant. We conclude that they are formed in an expanding envelope surrounding the whole system.

4. The Balmer lines.

There is an evident Balmer progression, the RV of Hα ranging between −28 and −38 km/s and those of the other lines becoming regularly less negative until $n = 9$ (Fig. 3). Hα is clearly associated with the M star between phases 0.0 and 0.16 and with the companion between phases 0.5 and 1.0, i.e. it shows the same behavior as H and K Ca II (Fig. 4a). Hβ presents the same behavior but the RV's are more scattered.

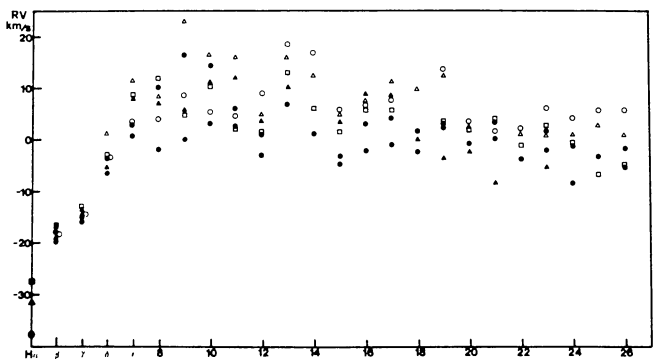

FIGURE 3. Radial velocity progression for the Balmer lines at different phases: 0.89(Δ), 0.90(•), 0.91(Δ), 0.92(□), 0.95(o).

Hγ and Hδ behave similarly but their RV curve is steeper and their RV's more positive, a consequence of the already mentioned Balmer progression. For $n > 15$ the Balmer lines show the same behavior although with more positive velocities and larger scatter (Fig. 4b).

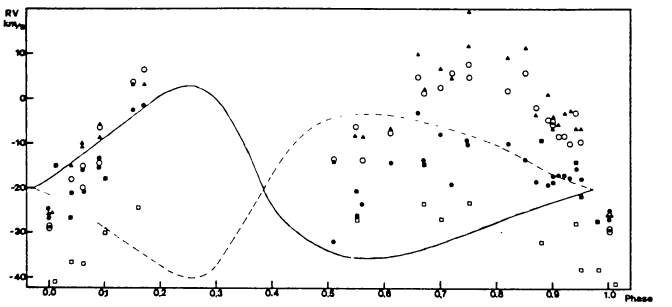

FIGURE 4a. Radial velocities of the Balmer absorption lines Hα(□), Hβ(■, red plates, • blue plates) Hγ(o) and Hδ(Δ). The orbital velocity curve (Wright 1977) is plotted for comparison.

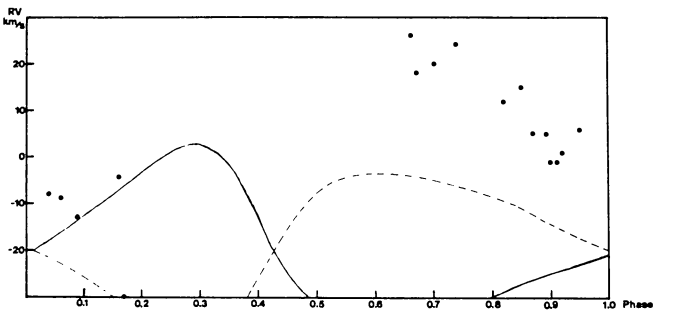

FIGURE 4b. Average radial velocity of the Balmer lines with $n > 15$. The orbital radial velocity curve is plotted for comparison.

The violet and red emission wings of Hα and Hβ have symmetric RV relatively to the velocity of the system: they are equal to about 80 km/s and do not show appreciable variation with the phase (Fig. 4c). The ratio R/V of the intensity of the emission wings is always less than one. These data suggest that the hydrogen emissions are formed in a extended rotating envelope surrounding the whole system.

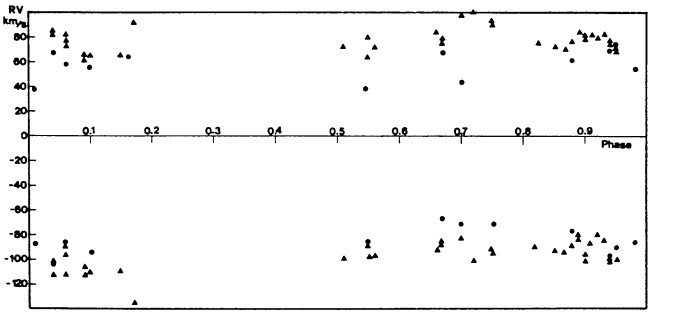

FIGURE 4c. Radial velocities of the violet and red emission wings of Hα(•) and Hβ(Δ).

However, the fact that the emissions at Hα become fainter at mid-eclipse indicate also the presence of an important contribution to the emissions from gas in the vicinity of the companion, maybe located in the first lagrangian point.

5. Permitted and forbidden Fe II emissions.

Their radial velocity curve is clearly associated with the M supergiant. We observe a systematic difference between the RV's of the permitted and forbidden lines: RV Fe II - RV [FeII] ranging between -7 and -10 km/s; it is more evident especially at phases 0.5 and 0.82 (Fig. 5). The other forbidden lines give RV's more negative than those of Fe II by about 5 km/s. The only exception is [NiII], which gives an almost constant velocity of -60 km/s. The Ti II absorption lines at $\lambda < 4000$ A seem to be associated with the M star between phases 0.0 and 0.16 and with the companion at phases between 0.5 and 0.8 (similar behavior to the H and K lines); their RV's, however, are more positive by 10 to 15 km/s than both the M star and the companion, just as are those of the upper members of the Balmer series. This is an indication that the outer layers, where the strongest lines are formed, are expanding, while the lower layers are falling back.

According to Peery (1969), the radial velocity of the iron emissions is constant and equal to the γ velocity. However, his data for the Fe II lines cover only a small interval of the orbital velocity curve, around phases 0.70-0.80.

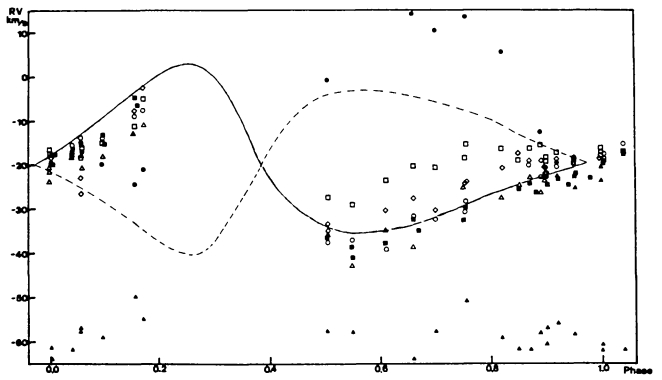

FIGURE 5. Radial velocities of the emission lines of FeII(◇), [FeII](□), [SII](△), [NiII](△), of the absorption lines of TiII for λ >4000 A(○) and for λ <4000 A(●), and for the average radial velocities of the lines of CaI (λ 4226 excluded), TiI, VI, CrI, MnI and FeI(■). Again the orbital velocity curve is plotted for comparison.

Table 3 gives the intensity ratio 4243 [FeII]/4233 Fe II. This ratio of the intensity of the forbidden and permitted iron lines may give an indication of the density and dilution of radiation of the hot star (Viotti 1976) in the regions where these lines are formed, if the following hypotheses are verified: the emitting region is homogeneous and optically thin for the emission lines and the permitted and forbidden lines are formed in the same volume. However these conditions are probably not verified as indicated by the difference in radial velocity of the permitted and forbidden Fe II emission lines.

6. Radial velocities of the Na I and CaI lines.

These are shown in Fig. 6. It is evident that, as expected, they follow the radial velocity curve of the M star. However, at phases 0.04-0.17 they are more negative by 5 km/s, and at phase 0.0-0.02 are more negative by 20 km/s. Only at a phase of about 0.7 a second component with velocity equal to the γ velocity is observable, probably because at that phase the separation between γ velocity and M star velocity is maximum. Unfortunately, we do not have observations around phase 0.25, when the separation is also maximum, to check our interpretation.

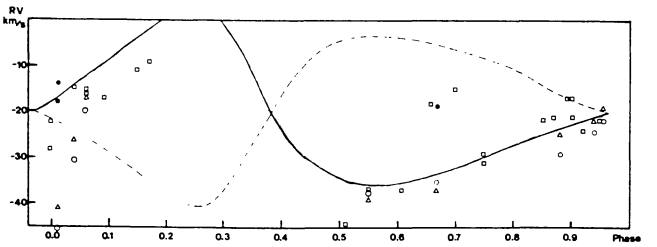

FIGURE 6. Radial velocities of 4226 CaI(□) and of the NaI D lines (○ λ 5889, △ λ 5895), second component of the NaI lines (●). Again the orbital velocity curve is plotted for comparison.

7. The profiles of selected lines *versus* the phase.

The Figures 7a-h show the profiles of the Balmer lines, CaII and CaI lines and the region of 4471 HeI at different phases. The spectra obtained by subtracting the spectrum at phase 0.0, i.e. a pure M-type spectrum from the composite spectra at the other phases, are given in Figures 8a-d. These figures give Sp(B+M) − Sp(M) = Sp(B).

We may make the following comments in Figure 7: The emission wings of Hα and Hβ disappear almost completely at phase 0.0, while they are strong at phases 0.94 and 0.04. There is the same behavior at Hγ and Hδ whose emissions disappear completely at phase 0.0. This behavior-as said above-suggests the presence of an envelope rotating at 80 km/s and observable at all phases, plus the contribution of a concentration near L_1, whose emission disappears at mid-eclipse, and contributes to the intensity of the lines at the other phases.

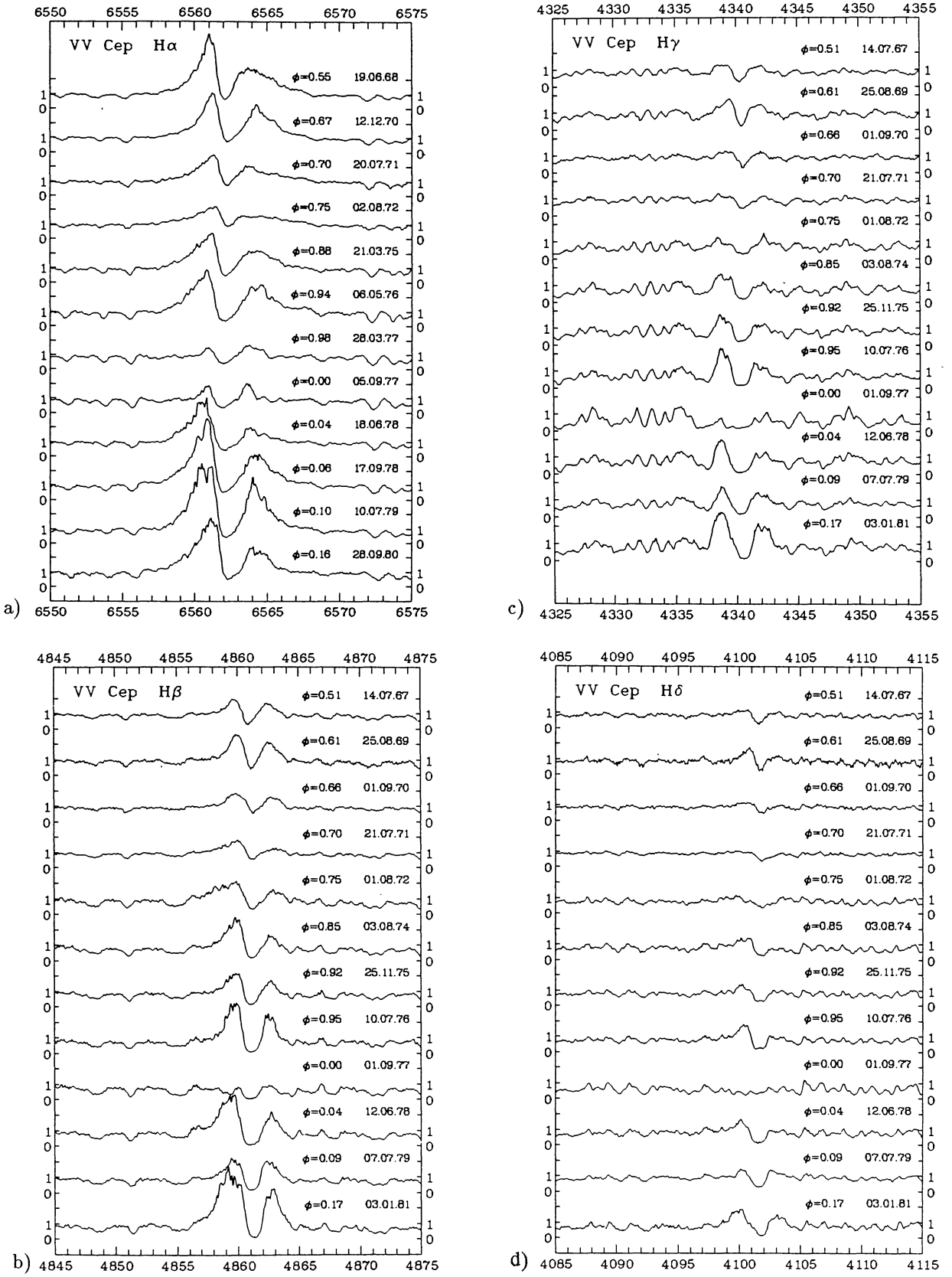

FIGURE 7. The normalized spectrum of VV Cephei at different phases. a) the region of Hα; b) the region of Hβ; c) the region of Hγ; d) the region of Hδ; e) the region of H 7 and H CaII; f) the region of K CaII; g and g') the region of 4226 CaI, 4233 FeII and 4243 [FeII]; h) the region of 4471 HeI.

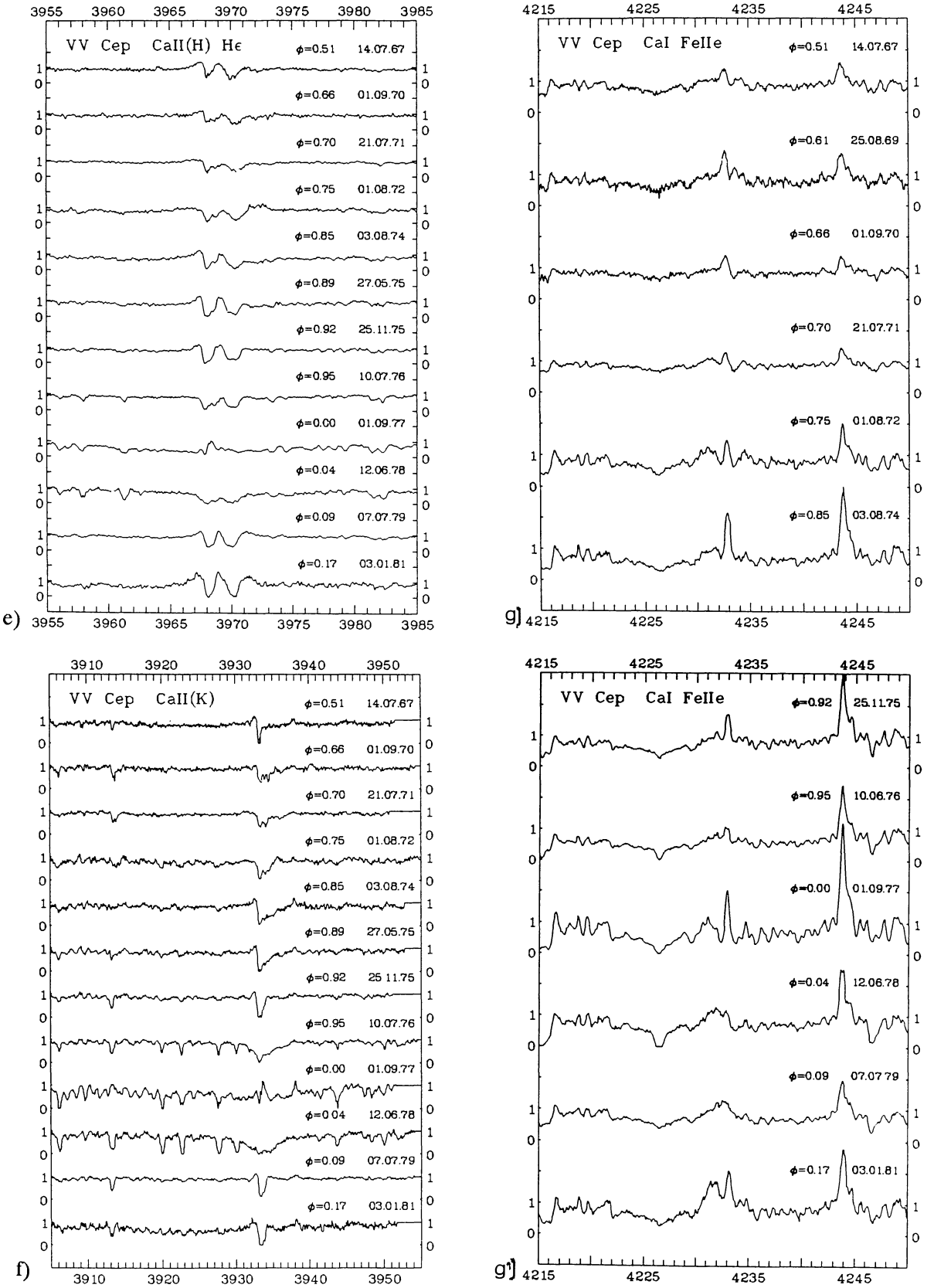

FIGURE 7. *(continued)*

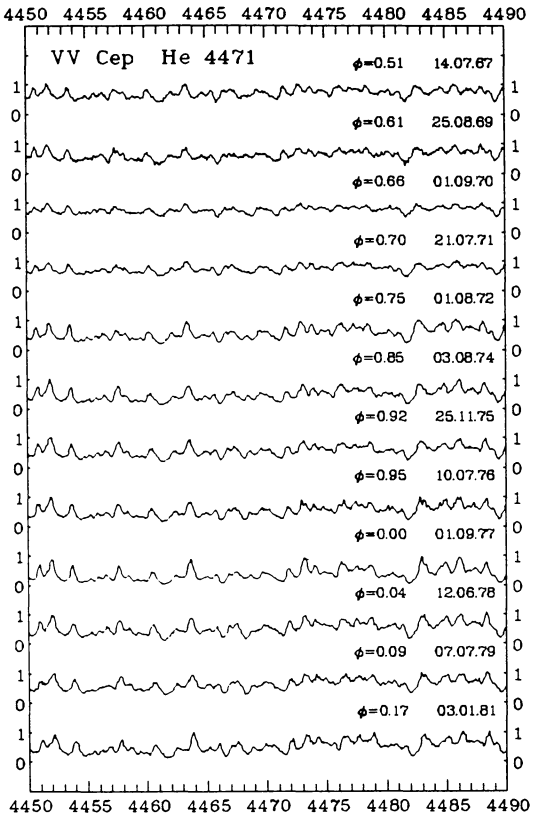

FIGURE 7h.

The H and K lines of Ca II disappear almost completely at phase 0.0 because the continuum of the M star is too faint to show these broad shallow absorptions; only a sharp P Cygni profile formed in the M chromosphere is observable.

The region of 4227 CaI, 4233 Fe II and 4243 [FeII] shows that the Ca I line is filled by the blue continuum of the companion, and becomes strong when its light is partially or completed eclipsed. At phases 0.92 and 0.09, there is evidence of atmospheric eclipse, as indicated by the sharp absorption core.

In the region of 3933 Ca II, where many lines typical of the spectrum of the M star are present, one observes the effect on the M spectral lines of the presence of the B continuum, which fills all the lines except at phases 0.95 to 0.04. In the region 4450-4490, on the contrary, the effect of the filling of the M lines from the B continuum is almost negligible, as expected.

Evidence for the filling of the M spectral lines by the B continuum at different wavelengths is also given by the variation in the central intensity of several absorption lines typical of the M spectrum. The variation is small in the spectral range 6000-6500 A and is much more evident around 4000 A (Fig. 9).

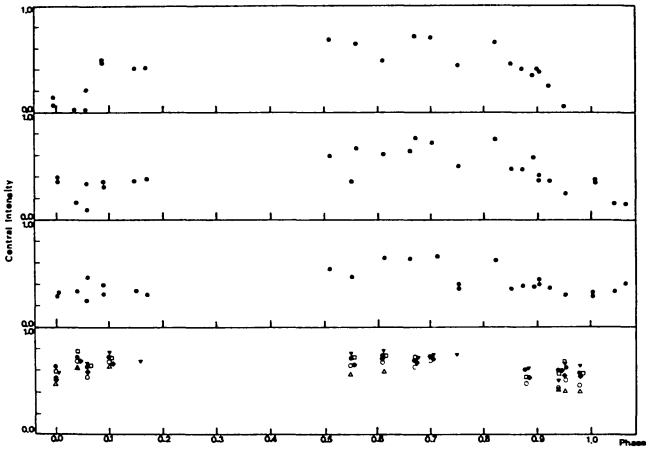

FIGURE 9. The variation with the phase of the central intensities of several lines typical of the M2 spectrum placed in different spectral regions. The filling of the lines by the continuum of the companion is evident in the blue region of the spectrum, while is almost undetectable in the red region. From top to bottom: 4077 SrII, 4246 ScII, 4468 TiII, 5426 TiI(Δ), 6039 VI(□), 6082 FeI(•), 6126 TiI(○), 6325 TiI(◇), 6531 VI(▽).

Figure 8 shows the difference of the normalized spectra at various phases minus that at phase 0.00. i.e. Sp(B+M)−Sp(M), the subtraction giving the pure spectrum of the companion. We make the following comments: The line at 4471.5 can be identified with 4471.68 Fe I, multiplet 2, formed in the spectrum of the M star as indicated by its radial velocity variations. There is no evidence at all of the presence of 4471 He I. Only the line 4472.9 has radial velocity indicating that it is formed in the spectrum of the companion and can be identified with Fe II, multiplet 37.

The difference Sp(B+M) −Sp(M) in the region 4215-4250 gives two spurious absorptions at 4233 and 4243, which are just due to the fact that the two emissions at phase 0.0 are stronger than at the other phases (probably due to the fact that the continuum is fainter during the eclipse). The same spurious absorption is observable, for the same reason, at Hα at phase 0.98. One should note the complete disappearance of a typical line of the M spectrum, 4227 Ca I.

8. Determination of the fluxes of the two stars.

We have used the method applied for the first time by Christie & Wilson (1935) to Zeta Aurigae for deriving the ratio between the fluxes of the two stars.

By comparing the equivalent widths W of selected regions in the composite spectrum (B+M) and in the pure M spectrum observed during totality, we obtain the ratio of the stellar fluxes $\alpha = F(\mathrm{B})/F(\mathrm{M}) = W(\mathrm{M})/W(\mathrm{BM}) - 1$.

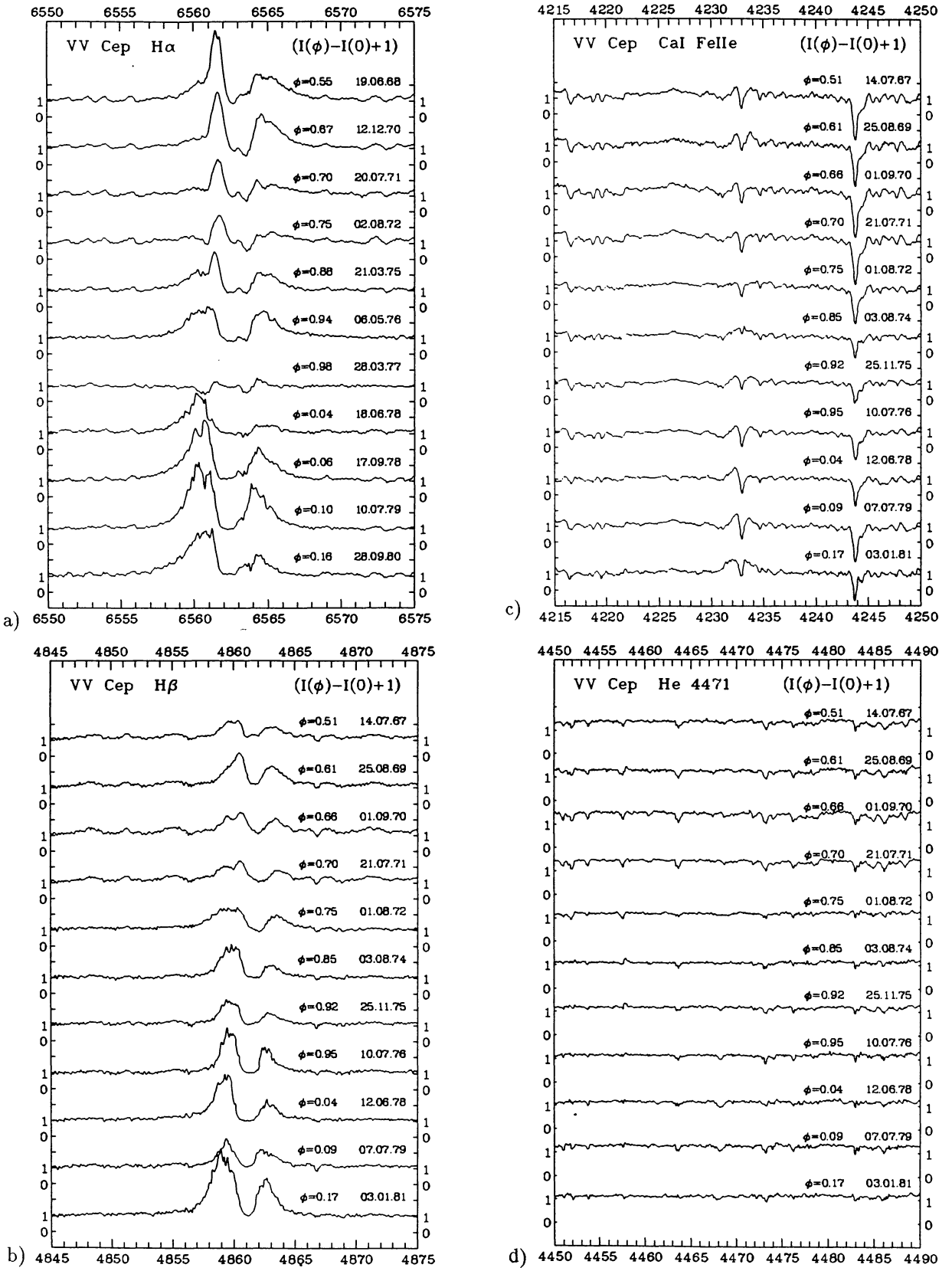

FIGURE 8. The difference between the normalized spectra at any phase and at phase 0.0 for the regions of Hα(a); H(β)(b); 4226 CaI (note that the absorptions at 4233 and 4243 are spurious and due to the fact that the emissions at phase 0.0 are stronger than at the other phases, probably just because the continuum is fainter at phase 0.0) (c); the region 4450-4490 A: there is no evidence of the presence of 4471 HeI (d).

We have chosen regions where neither strong lines of the hot star nor strong low excitation lines, which could be formed in the circumstellar envelope are expected. The results are given in Figure 10, where they are plotted together with the same data derived by Goedicke and by Peery for the eclipse of 1935-37. They used single lines, while we have used extended regions of several angstroms in order to obtain a higher precision (Tab. 4). However, the errors are high, especially because of the difficulty in tracing the continuum in a consistent way at phase 0.0 and at phases when the two spectra are present.

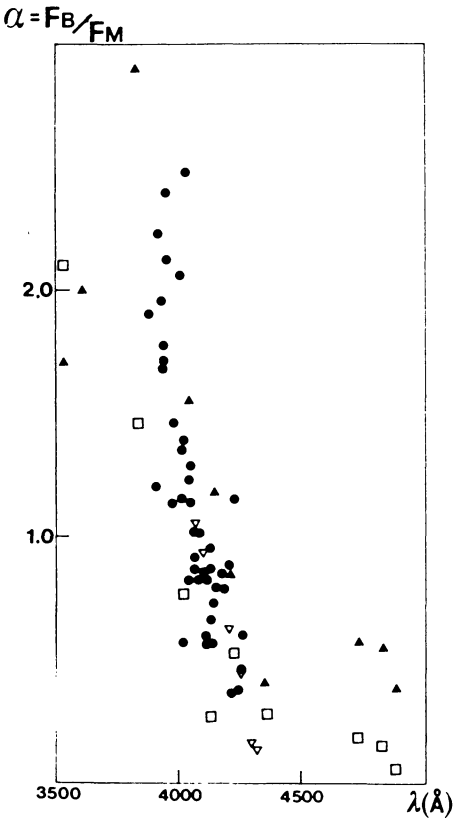

FIGURE 10. The values of α plotted *versus* the wavelength. Hack from phases 0.0 and 0.70-0.75(△); Hack from phases 0.0 and 0.16(□), Goedicke(•), Peery(▽).

By assuming that the fluxes of the two stars can be approximated by the Planck law, the differences in the reciprocal of the color temperatures of the two stars can be derived, either by comparing the values of α at two different wavelengths, or by assuming the ratio of the two radii derived by the light curve and solving the equation for the wavelength where $F(\mathrm{B})/F(\mathrm{M})$ is equal to 1 (that is at about 4050 Å). The value for $T(\mathrm{B})$ strongly depends upon the value assumed for $T(\mathrm{M})$. For this reason we have attempted to obtain a direct determination of the color temperature for VV Cephei using the IR colors given in the IRAS catalogue (Gezari *et al.* 1987). We have corrected them for reddening ($E(B-V) = 0.40$, Hack *et al.* 1989) and compared the infrared flux of VV Cephei with that of α Orionis. It turns out that the energy distribution of VV Cephei is strictly similar to that of α Orionis, but its maximum falls at about 1.4 μm while that of α Ori falls at 1 μm (Fig. 11) suggesting that the temperature of VV Cep is slightly lower than that of α Ori.

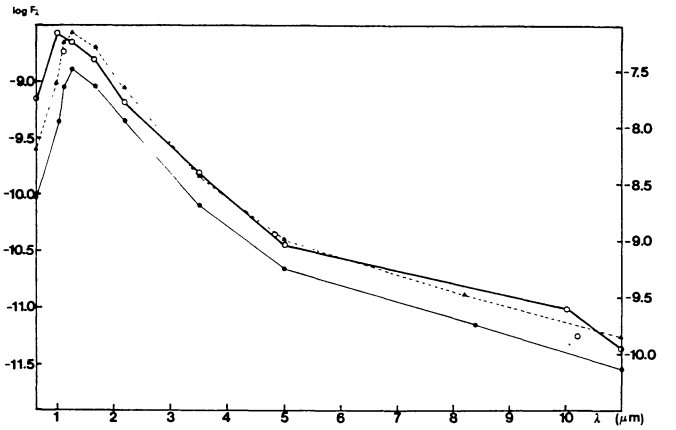

FIGURE 11. The log of the infrared fluxes of α Orionis(o) (right ordinate scale) and of VV Cephei (left ordinate scale), observed (•) and dereddened for $E(B-V) = 0.40$(△) *versus* the wavelengths (data from IRAS Catalogue, 1987).

The results of the determination of the color temperature $T(\mathrm{B})$ are given in Table 5, assuming for $T(\mathrm{M})$ both the mean value for spectral type M2 I, $T = 3200$ K and for $T = 3000$ K.

The temperature of the companion has been derived by comparing the values of α at 4000 Å and 4900 Å, and at 3900 Å and 4800 Å. At lower wavelengths the spectra are underexposed and the measurements are uncertain; at higher wavelengths the difference between the spectra B+M and pure M are smaller than the measurement errors. However, we have attempted to use the mean values of all the determinations made by us and by previous authors $\alpha(3600) = 1.55 +/- 0.20$ and $\alpha(4800) = 0.26 +/- 0.05$, and we have found that $T(\mathrm{B})$ ranges between 11770 K and 6500 K with the most probable value being equal to 8197 K, by assuming $T(\mathrm{M}) = 3200$ K.

This results, along with the fact that no trace of helium lines is detectable in the optical spectrum (see the previous section), confirms our determination of the spectral type from the UV IUE data, i.e. A0 II.

The other results obtained by assuming the two values for $T(\mathrm{M})$ are summarized in Table 5.

The two fluxes have the same value at about 4050 A. From the relation

$$R(\mathrm{B})^2 \mathrm{B}[4050,\ T(\mathrm{B})]/R(\mathrm{M})^2[\mathrm{B}(4050,\ T(\mathrm{M})]$$

and assuming $R(\mathrm{M}) = 1600$ solar radii, $R(\mathrm{B}) = 13$ solar radii (Wright, 1977) and $T(\mathrm{M}) = 3000$ K, a value of

T(B) = 15000 K is found, which is not compatible with the complete absence of He I lines. If on the contrary, we assume T(B) of about 10000 K and derive the ratio of the two radii, it results that for R(M) = 1600, R(B) is equal to 25 solar radii.

It is impossible to ascertain if these data refer to the photosphere of the companion or if we are observing just a thick disk around it.

9. Conclusion.

The main results of this study are the following: The radial velocities of the H and K Ca II lines and of the Balmer lines seem to indicate an association with the M giant at phases included between 0.0 and 0.17, and with the companion at phases included between 0.5 and 0.9. The permitted and forbidden lines of Fe II are clearly associated with the M star, a result which disagrees with those obtained by previous authors, although the latter are relative to a more restricted interval of the period.

The temperature of the companion derived by the ratio between the fluxes of the two stars, and the absence of 4471 HeI line confirms that the spectrum of the companion (star or accretion disk around it) is a late B or early A.

References

Christie W.H., Wilson O.C. 1935, ApJ 81, 246

Gezari D.Y., Schmitz M., Mead J.M. 1987, Catalog of Infrared Observations, Part I-Data, NASA Reference Publication 1196

Goedicke V. 1939, Publ. Observatory of the University of Michigan, Vol. 8, No.1

Hack M., Engin S., Yilmaz N. 1989, A&A 225, 143

Peery B.F. 1966, ApJ 144, 672

Reimers D., Schroeder K.-P. 1989, A&A 214, 261

Struve O. 1944, ApJ 99, 70

Viotti R. 1976, ApJ 204, 293

Wright K.O. 1970, Vistas in Astron. 12, 147

Wright K.O. 1977, J.R.A.S.C. 71, 152

Wright K.O., Larson S.J. 1969, in: Mass Loss from stars, M. Hack Ed. (D. Reidel, Dordrecht) p. 198

TABLE 1. *The observations.*

Blue Plates	Date	JD	Phase	Observer
W 3593	July 14,1967	243 9686.5	0.51	Faraggiana
W 4330	June 19,1968	244 0027.5	0.55	"
W 4465	Aug. 13,1968	0082.5	0.56	Hack
W 4936	Aug. 25,1969	0459.5	0.61	Faraggiana
GB 345	Sep. 1,1970	0831.3	0.66	Hack,Stalio
GB 744	Dec. 12,1970	0933.3	0.67	Aydin,Hack,Stalio
GB1237	July 21,1971	1154.6	0.70	Faraggiana,Hack
GB1685	Dec. 11,1971	1297.4	0.72	Faraggiana,Stalio
GB2033	Aug. 1,1972	1531.5	0.75	Engin,Faraggiana,Hack
GB2056	Aug. 6,1972	1536.6	0.75	" " "
GB2715	Dec. 28,1973	2045.4	0.82	Faraggiana,Hack
GB2915	Aug. 3,1974	2262.5	0.85	Faraggiana
GB3222	Jan. 1,1975	2414.3	0.87	Faraggiana, Hack
GB3374	May 27,1975	2560.5	0.89	Faraggiana
GB3397	July 25,1975	2619.5	0.90	"
GB3398	July 26,1975	2620.6	0.90	"
GB3426	Sep. 21,1975	2677.5	0.91	Hack
GB3503	Nov. 25,1975	2742.4	0.92	Faraggiana
GB3608	Feb. 15,1976	2824.5	0.93	"
GB3649	May 7,1976	2906.4	0.94	Stalio
GB3713	July 10,1976	2970.5	0.95	Faraggiana
GB4113	Sep. 1,1977	3388.5	0.00	Aydin,Castelli,Faraggiana
GB4125	Sep. 3,1977	3390.4	0.00	" " "
GB4133	Sep. 4,1977	3391.5	0.00	" " "
GB4572	June 12,1978	3672.6	0.04	Faraggiana
GB4723	Sep. 16,1978	3768.4	0.06	"
GB4736	Sep. 17,1978	3769.5	0.06	"
GB5366	July 7,1979	4062.6	0.09	"
GB5379	July 9,1979	4064.6	0.09	"
GB5988	Sep. 26,1980	4509.4	0.15	"
GB6000	Sep. 29,1980	4512.3	0.16	"
GB6317	Jan. 3,1981	4608.2	0.17	"
Red Plates				
W 4370	June 19,1968	0027.6	0.55	Faraggiana
W 4935	Aug. 25,1968	0459.5	0.61	"
W 5316	Dec. 12,1970	0933.3	0.67	Hack
GB1229	July 20,1971	1153.5	0.70	Faraggiana,Hack
GB2035	Aug. 2,1972	1532.5	0.75	Engin,Faraggiana,Hack
GB2040	Aug. 3,1972	1533.6	0.75	" " "
GB3338	Mar. 21,1975	2493.7	0.88	Selvelli,Stalio
GB3400	July 27,1975	2621.4	0.90	Faraggiana
GB3645	May 6,1976	2905.6	0.94	Stalio
GB3650	May 9,1976	2908.5	0.94	"
GB3719	July 12,1976	2972.6	0.95	Faraggiana
GB3955	Mar. 28,1977	3231.6	0.98	Hack
GB4140	Sep. 5,1977	3392.5	0.00	Castelli,Faraggiana
GB4583	June 18,1978	3678.5	0.04	Faraggiana
GB4735	Sep. 17,1978	3769.5	0.06	"
GB5384	July 10,1979	4065.5	0.10	"
GB5996	Sep. 28,1980	4511.4	0.16	"

TABLE 2. *Orbital and wind parameters of VV Cephei.*

a sin i (km)	$19.46\ 10^8$	
P(days)	7430	
mass ratio m(M)/m(B)	~1 (Wright 1977)	
v(wind)(km/s)	20 (CS H & K CaII)	20(Hα)
Phase displacement ΔT (days)	1860	
Δ T/P	0.25	0.25(Hα)
K(km/s)	19.4	
K(wind)(km/s)	20	
K(wind)/K	1	
R (solar radii)	1600	
$a \sin i / R^*$	1.73	
Wind flow time t for 1 R^* (days)	648	
t/P	0.087	
v_{wind}/K	1	
Shell distance V(wind) $\Delta T/R^*$	2.87 R_M	

TABLE 3. *The intensity ratio 4243 [FeII]/4233 FeII.*

Phase	I(4243)/I(4233)	Phase	I(4243)/I(4233)
0.00	1.62	0.70	1.09
0.04	1.89	0.75	1.34
0.06	1.64	0.82	1.14
0.09	1.41	0.85	1.38
0.15	1.44	0.87	1.35
0.17	1.31	0.89	1.49
0.51	1.13	0.90	1.46
0.57	1.60	0.92	1.51
0.61	0.92	0.95	1.74
0.66	1.01		

TABLE 4. *Spectral regions used for the determination of α.*

Interval (A)	Average equivalent widths and quadratic errors 0.70-0.75		0.15-0.17		0.00		α 0.0/0.7	0.0/0.16
3502-3540	0.209	0.010	0.181	0.014	0.563	0.037	1.69	2.11
3615-3645	0.185	0.043	0.096	0.068	0.555	0.104	2.00	4.78
3810-3826	0.138	0.026	0.222	0.040	0.542	0.045	2.92	1.44
4050-4070	0.169	0.045	0.243	0.039	0.431	0.015	1.55	0.77
4151-4171	0.148	0.041	0.250	0.014	0.322	0.060	1.17	0.29
4206-4232	0.233	0.101	0.286	0.029	0.433	0.021	0.86	0.51
4352-4405	0.357	0.061	0.393	0.020	0.499	0.059	0.40	0.27
4710-4751	0.280	0.052	0.370	0.017	0.442	0.004	0.58	0.19
4800-4836	0.272	0.049	0.370	0.028	0.421	0.002	0.55	0.13
4875-4899	0.286	0.050	0.376	0.030	0.396	0.018	0.38	0.05
6615-6642	0.095	0.006			0.137		0.44	

TABLE 5. *Determination of the temperature of the companion.*

$\alpha(4000)/\alpha(4900) = 1.12/0.26$ gives $1/T(B) - 1/T(M) = -2.21\ 10^{-4}$

Assuming T(M)= 3200 K , T(B) = 10945 K

T(M)= 3000 K , T(B) = 8912 K

$\alpha(3900)/\alpha(4800) = 1.30/0.25$ gives $1/T(B) - 1/T(M) = -2.38\ 10^{-4}$

Assuming T(M) =3200 K ,T(B) = 13480 K

T(M) = 3000 K, T(B) = 10470 K